lncRNA VIM-AS1 promotes cell proliferation, metastasis and epithelial-mesenchymal transition by activating the Wnt/β-catenin pathway in gastric cancer

JIN-GUI SUN[1], XIAO-BO LI[2], RUI-HONG YIN[2] and XIAO-FENG LI[3]

[1]Department of Oncology, Shouguang People's Hospital, Shouguang, Shandong 262700;
[2]Department of Gastroenterology, First People's Hospital of Jinan, Jinan, Shandong 250011;
[3]Yulin Cancer Diagnosis and Treatment Center, The First Hospital of Yulin, Yulin, Shaanxi 719000, P.R. China

Received December 6, 2019; Accepted July 28, 2020

DOI: 10.3892/mmr.2020.11577

Abstract. The present study aimed to explore the biological functions and molecular mechanisms of the long non-coding RNA VIM antisense RNA 1 (VIM-AS1) in gastric cancer (GC). The expression of VIM-AS1 was analyzed in tissues from patients with GC and GC cell lines by reverse transcription-quantitative (RT-q)PCR. The relationship between VIM-AS1 expression and overall survival time of patients with GC was also assessed. To determine the biological functions of VIM-AS1, Cell Counting Kit-8 assay, colony formation assay, flow cytometry, wound healing assay and Transwell assay were employed. The targeting relationship among VIM-AS1, microRNA (miR)-8052 and frizzled 1 (FZD1) was verified by the dual luciferase reporter gene assay. The underlying molecular mechanism of VIM-AS1 on GC was determined by RT-qPCR and western blotting. In addition, tumor formation was detected in nude mice. The results of the present study demonstrated that VIM-AS1 was highly expressed in GC tissues and cells. In addition, VIM-AS1 expression was demonstrated to be closely related to the prognosis of patients with GC. Notably, silencing VIM-AS1 inhibited the proliferation, migration and invasion, and enhanced apoptosis of AGS and HGC-27 cells. Silencing VIM-AS1 significantly increased the protein expression levels of cleaved caspase-3, Bax and E-cadherin, but decreased the protein expression levels of Bcl-2, N-cadherin, vimentin, matrix metalloproteinase (MMP)-2, MMP-9, β-catenin, cyclin D1, C-myc and FZD1. Additionally, silencing VIM-AS1 inhibited tumor growth in nude mice. Cumulatively, the present study demonstrated that VIM-AS1 may promote cell proliferation, migration, invasion and epithelial-mesenchymal transition by regulating FDZ1 and activating the Wnt/β-catenin pathway in GC.

Correspondence to: Dr Xiao-Feng Li, Yulin Cancer Diagnosis and Treatment Center, The First Hospital of Yulin, 93 Yuxi Avenue, High Tech Zone, Yuyang, Yulin, Shaanxi 719000, P.R. China
E-mail: lxfyx357@163.com

Key words: gastric cancer, VIM antisense RNA 1, proliferation, metastasis, epithelial-mesenchymal transition, Wnt/β-catenin pathway

Introduction

Gastric cancer (GC) is one of the most common malignancies and the second leading cause of cancer-related mortality worldwide (1). Reportedly, ~380,000 new cases of GC are recorded every year in China alone (2). Despite therapy for GC improving in recent years, the overall 5-year survival rate remains unsatisfactory (3). Therefore, it is critically important to explore target genes and to understand their underlying molecular mechanisms for the prognosis and treatment of GC.

Long non-coding RNAs (lncRNAs) are a group of transcripts >200 nucleotides long that lack a protein-coding function (4). An increasing number of studies have indicated that lncRNAs exert important functions in the progression of cancer by regulating the proliferation, apoptosis, cell cycle, migration and invasion of tumor cells (5-7). A number of studies have demonstrated that lncRNAs serve a regulatory role in GC as oncogenes or tumor suppressor genes (8,9). For example, lncRNA human ovarian cancer specific transcript 2 has been reported to accelerate cell proliferation and metastasis in GC (10). In addition, Pan *et al* (11) observed that lncRNA differentiation antagonizing non-protein coding RNA promoted GC cell proliferation and invasion by activating spalt-like transcription factor 4. In recent years, lncRNA VIM antisense RNA 1 (VIM-AS1) has been reported to promote cell migration and invasion through regulating the epithelial-mesenchymal transition (EMT) in colorectal cancer and preeclampsia (12,13). However, to the best of our knowledge, the effect of VIM-AS1 on GC remains to be determined.

The Wnt/β-catenin pathway has been reported to be involved in the occurrence and development of GC (14). Numerous lncRNAs may regulate the proliferation and metastasis of several types of tumor cells through modulating the Wnt/β-catenin pathway (15). For example, growth-arrest associated lncRNA 1 has been reported to inhibit the growth of GC via inactivation of the Wnt/β-catenin pathway (16). Another study reported that the downregulation of lncRNA

TP73 antisense RNA 1 (TP73-AS1) inhibited the proliferation and invasion of GC cells by regulating the Wnt/β-catenin pathway (17). However, to the best of our knowledge, it remains unknown as to whether VIM-AS1 affects GC progression through modulating the Wnt/β-catenin pathway.

In the present study, the role of VIM-AS1 in GC and its underlying molecular mechanisms were explored. The results of the present study demonstrated that VIM-AS1, which is considered to be an oncogene, promoted cell proliferation, migration, invasion and EMT by regulating frizzled 1 (FZD1) and activating the Wnt/β-catenin pathway in GC. Thus, this study may provide a strategy and facilitate the development of lncRNA-directed diagnostic and therapeutic strategies against GC.

Materials and methods

Patients and clinical tissue samples. A total of 50 GC tissues and 30 adjacent non-tumor tissues (located >5 cm from the tumor) were collected from 50 patients (24 men and 26 women; age range, 26-70 years; mean age, 47.7±6.3 years) who underwent surgical resection at Shouguang People's Hospital (Shouguang, China) between April 2014 and March 2019. None of the patients received radiotherapy or chemotherapy before the operation. Diagnosis was confirmed in all patients through pathological examination. GC tissues and adjacent non-tumor tissues were stored in liquid nitrogen until use. This study was approved by the Ethics Committee of Shouguang People's Hospital and all patients provided written informed consent. The clinical characteristics of the patients are presented in Table I.

Cell culture and transfection. The human GC cell lines AGS and HGC-27, and the normal gastric mucosa epithelial cell line GES-1, were purchased from the Cell Bank of Chinese Academy of Sciences. AGS and HGC-27 cells were cultured in RPMI-1640 medium (Gibco; Thermo Fisher Scientific, Inc.), whereas GES-1 cells were cultured in DMEM (Gibco; Thermo Fisher Scientific, Inc.) supplemented with 10% FBS (Gibco; Thermo Fisher Scientific, Inc.), 100 μg/ml streptomycin (Sigma-Aldrich; Merck KGaA) and 100 U/ml penicillin sodium (Sigma-Aldrich; Merck KGaA). All cells were cultured in a humidified 5% CO_2 incubator at 37˚C. AGS and HGC-27 cells were harvested at 70-80% confluence and were then transfected with 40 nM VIM-AS1 small interfering (si)RNA (si-VIM-AS1), VIM-AS1 negative control siRNA (si-NC), miR-8052 mimics, miR-8052 mimics negative control (mimics NC), miR-8052 inhibitor and miR-8052 inhibitor negative control (inhibitor NC) using Lipofectamine® 3000 (Invitrogen; Thermo Fisher Scientific, Inc.), according to the manufacturer's protocol. The cells were transfected for 24 h at 37˚C and stored for subsequent experiments. Untransfected AGS and HGC-27 cells served as the control cells. si-VIM-AS1, si-NC, miR-8052 mimics, mimics NC, miR-8052 inhibitor and inhibitor NC were designed and synthesized by Sangon Biotech Co., Ltd. The sequences used were as follows: si-VIM-AS1, 5'-GCTTGCAGAATCTTTGCTTTT-3'; si-NC, 5'-UUCUCCGAACGUGUCACGUTT-3'; miR-8052 mimics, 5'-CGGGACUGUAGAGGGCAUGAGC-3'; mimics NC, 5'-UUCUCCGAACGUGUCACGUTT-3'; miR-8052 inhibitor, 5'-GCUCAUGCCCTCTACAGUCCCG-3'; and inhibitor NC, 5'-CAGUACUUUUGUGUAGUACAA-3'.

Cell Counting Kit-8 (CCK-8) assay. The effects of VIM-AS1 on GC cell proliferation were assessed using the CCK-8 kit (Beyotime Institute of Biotechnology), according to the manufacturer's instructions. Briefly, the transfected AGS and HGC-27 cells were seeded into a 96-well plate at a density of $1x10^4$ cells/well. Subsequently, 10 μl CCK-8 solution was added to each well at different time points, followed by incubation at 37˚C for 4 h. Finally, the optical density of each well at a wavelength of 450 nm was detected using a microplate reader.

Colony formation assay. After 24 h of transfection, AGS and HGC-27 cells ($1x10^3$) were plated into a 12-well plate and incubated in a humidified 5% CO_2 incubator at 37˚C. After 2 weeks of incubation, the cells were fixed in 4% paraformaldehyde at 37˚C for 20 min and stained with 0.1% crystal violet at 37˚C for 10 min. Subsequently, the numbers of cell colonies were calculated under a light microscope.

Flow cytometric analysis. The apoptotic ability of AGS and HGC-27 cells was evaluated by flow cytometry. Briefly, the transfected AGS and HGC-27 cells ($1x10^5$) were digested with trypsin and then resuspended in 1X binding buffer. Subsequently, 5 μl Annexin V-fluorescein isothiocyanate (FITC) and 5 μl propidium iodide from the Annexin V-FITC apoptosis kit (BD Biosciences) were added to the cell suspension and maintained in the dark for 15 min at room temperature. Early and late apoptosis were then detected by a FACSCalibur instrument (BD Biosciences) within 1 h of staining. The results were analyzed by FlowJo software (version 7.6.3; FlowJo LLC).

Wound-healing assay. The GC cell motility capacity was assessed by a wound-healing assay. The transfected AGS and HGC-27 cells ($3x10^5$ cells/well) were plated into a 6-well plate and incubated for 24 h at room temperature to form a 90% confluent monolayer. The cell layer was then scratched with a sterile plastic tip and washed with PBS. Thereafter, serum-free medium was added to each well, and the scratched monolayer was cultured for 48 h. The images were captured at 0 and 48 h after scratching under a light microscope, after which the wound-healing rate was calculated and recorded. The formula used to calculate the wound-healing rate was as follows: [wound width (0 h)-wound width (48 h)]/wound width (0 h) x100%.

Transwell assay. The migratory and invasive capabilities of AGS and HGC-27 cells were determined using Transwell chambers (Corning, Inc.), according to the manufacturer's protocol. For the migration assay, the transfected AGS and HGC-27 cells ($1x10^5$ cells/ml) in serum-free medium were seeded into the upper chamber. For the invasion assay, the transfected AGS and HGC-27 cells ($1x10^5$ cells/ml) were plated into the upper chamber, which was pre-coated with Matrigel at room temperature (BD Biosciences). Subsequently, 500 μl RPMI-1640 medium containing 10% FBS was added to the lower chamber and cells were cultured for 24 h in an incubator at 37˚C. The chambers were then removed, and the

Table I. Association between the expression of VIM-AS1 and the clinicopathological factors of 50 patients with gastric cancer.

Characteristics	Number of cases	VIM-AS1 expression	P-value
Age, years			
<50	23	5.155±1.422	0.481
≥50	27	5.049±1.736	
Sex			
Female	26	5.101±1.486	0.490
Male	24	5.095±1.716	
TNM stage			
I/II	17	4.471±0.682	<0.001[a]
III/IV	33	5.960±1.166	
Tumor size, cm			
>5	19	5.340±1.594	0.128
<5	31	4.950±1.586	
Lymph node metastasis			
Yes	35	5.998±1.177	<0.001[a]
No	15	4.031±0.861	
Distant metastasis			
Yes	13	6.683±1.016	<0.001[a]
No	37	4.597±1.188	
Histological differentiation			
High/middle	24	4.761±1.374	0.106
Low	26	5.409±1.724	

[a]P<0.001. VIM-AS1, VIM antisense RNA 1.

cells were fixed with 4% paraformaldehyde for 20 min at room temperature and stained with crystal violet for 10 min at room temperature. The numbers of migrating or invading cells were counted under a light microscope in five representative fields.

Dual luciferase reporter gene assay. TargetScan 7.2 (http://www.targetscan.org/vert_72/) and DIANA tools (http://carolina.imis.athena-innovation.gr/) were used to predict the targeted relationship among VIM-AS1, miR-8052 and FZD1. For the dual luciferase reporter gene assay, AGS and HGC-27 cells ($6x10^4$ cells/well) were co-transfected with PsiCHECK-2 luciferase plasmids (Promega Corporation) carrying VIM-AS1-wild-type (Wt) or VIM-AS1-mutant (Mut) 3'untranslated regions (UTRs) and miR-8052 mimics or mimics NC at 37˚C using Lipofectamine® 3000 (Invitrogen; Thermo Fisher Scientific, Inc.). In addition, FZD1-Wt or FZD1-Mut 3'UTRs and miR-8052 mimics or mimics NC were transfected into AGS and HGC-27 cells at 37˚C using Lipofectamine 3000. After 48 h of transfection, the luciferase activity was detected using a dual luciferase kit (Promega Corporation), according to the manufacturer's protocols. The firefly luciferase activity was normalized using *renilla* luciferase activity.

Reverse transcription-quantitative (RT-q)PCR. TRIzol® reagent (Invitrogen; Thermo Fisher Scientific, Inc.) was used to extract total RNA from GC tissues and cells. RNA was reverse transcribed to cDNA using Reverse EasyScript One-Step gDNA Removal and cDNA Synthesis SuperMix (Beijing Transgen Biotech Co., Ltd.). The conditions for reverse transcription were as follows: 25˚C for 5 min, 55˚C for 20 min and 85˚C for 5 min. Subsequently, qPCR was performed with a ABI 7500 Real-time PCR instrument (Applied Biosystems; Thermo Fisher Scientific, Inc.) using TransStart TipTop Green qPCR SuperMix (Beijing Transgen Biotech Co., Ltd.) with the following primer sequences: VIM-AS1, forward 5'-ACT GTAATGGACTCGTGGTG-3' and reverse 5'-CGTCGTGTT GTCCTGATG-3'; miR-8052, forward 5'-CGGGACTGTAGA GGGCATGAGC-3' and reverse 5'-AACAATTGGAGGGCT GCGG-3'; U6, forward 5'-GCTTCGGCACATATACTAAAA T-3', and reverse 5'-CGCTTCACGAATTTGCGTGTCAT-3'; β-catenin, forward 5'-TGCAGTTCGCCTTCACTATG-3' and reverse 5'-ACTAGTCGTGGAATGGCACC-3'; C-myc, forward 5'-CACAGCAAACCTCCTCACAG-3' and reverse 5'-GGATAGTCCTTCCGAGTGGA-3'; cyclin D1, forward 5'-GAGACCATCCCCCTGACGGC-3' and reverse 5'-TCT TCCTCCTCCTCGGCGGC-3'; and GAPDH, forward 5'-GCT CTCTGCTCCTCCTGTTC-3' and reverse 5'-ACGACCAAA TCCGTTGACTC-3. The results were analyzed using the $2^{-\Delta\Delta Cq}$ method (18). mRNA and lncRNA expression levels were normalized to the levels of GAPDH, whereas miRNA expression levels were normalized to U6. The RT-qPCR reaction conditions were as follows: Initial denaturation at 94˚C for 120 sec, followed by 40 cycles at 95˚C for 30 sec, 60˚C for

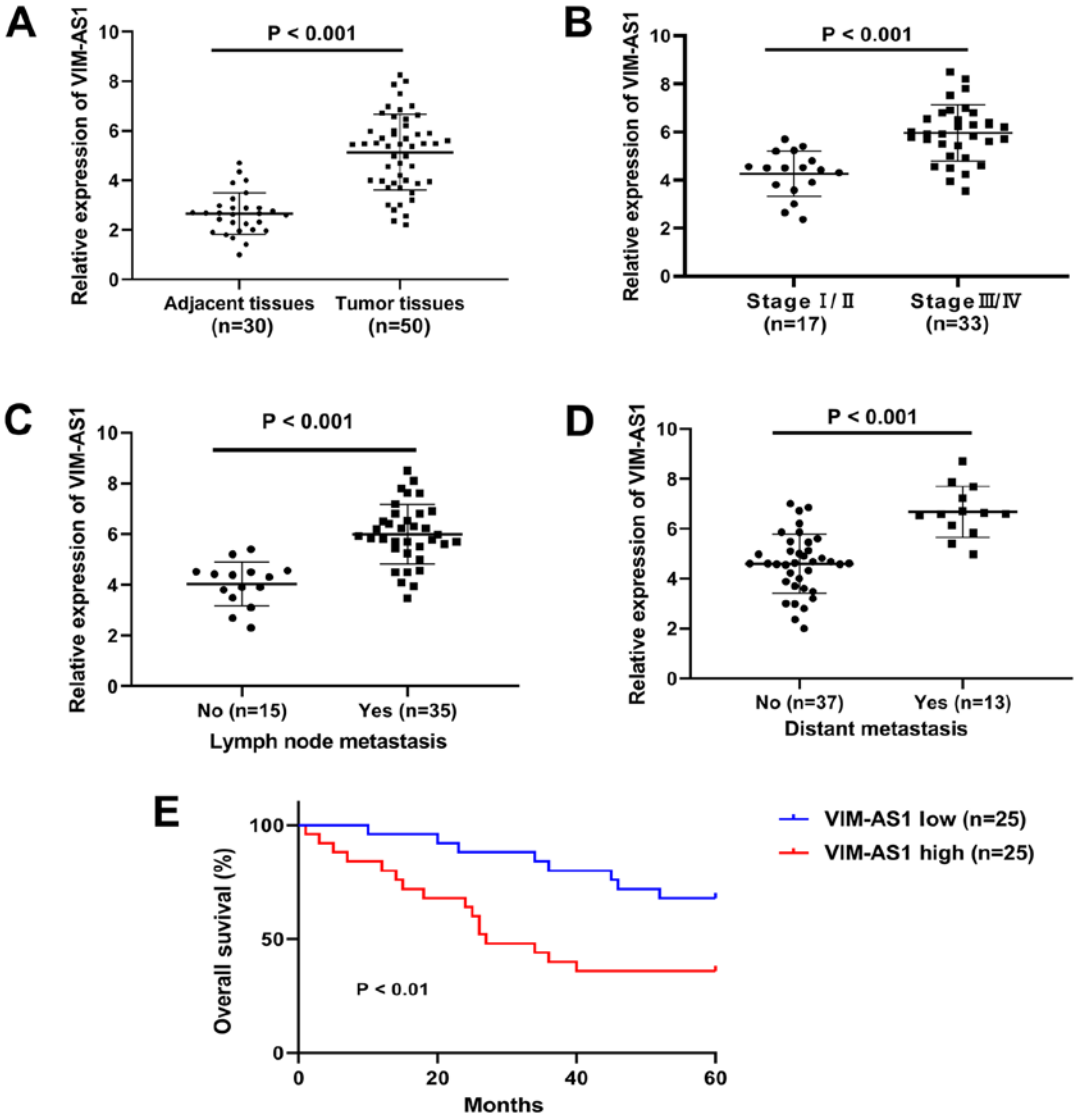

Figure 1. VIM-AS1 expression is upregulated in GC tissue and is associated with the prognosis of GC. (A) VIM-AS1 expression in GC tissues and matched cancer-adjacent tissues was detected by RT-qPCR. (B) VIM-AS1 expression in TNM stage I/II and III/IV tumors was measured by RT-qPCR. (C) VIM-AS1 expression was detected in tissues from patients with GC with or without lymph node metastasis by RT-qPCR. (D) VIM-AS1 expression was detected in tissues from patients with GC with or without distant metastasis by RT-qPCR. (E) Relationship between VIM-AS1 expression and overall survival time of patients with GC. VIM-AS1, VIM antisense RNA 1; GC, gastric cancer; RT-qPCR, reverse transcription-quantitative PCR.

30 sec, 72˚C for 90 sec, and a final extension step at 72˚C for 5 min.

Western blot analysis. Total protein was extracted from AGS and HGC-27 cells using RIPA lysis buffer (Beyotime Institute of Biotechnology). A BCA protein assay kit (Beyotime Institute of Biotechnology) was used to measure the protein concentrations. Protein samples (50 μg) were separated by 10% SDS-PAGE and were then transferred onto polyvinylidene difluoride (PVDF) membranes. Membranes were blocked with 5% non-fat milk for 2 h at room temperature, and incubated with the primary antibodies overnight at 4˚C. Subsequently, the PVDF membranes were incubated with the horseradish peroxidase-conjugated anti-rabbit IgG secondary antibody (1:5,000; cat. no. A3687; Sigma-Aldrich; Merck KGaA) and the anti-mouse IgG secondary antibody (1:5,000; cat. no. 2216; Cell Signaling Technology, Inc.) at room temperature for 1 h. Finally, the protein bands were visualized with an enhanced chemiluminescence kit (Beyotime Institute of Biotechnology) and analyzed with a Molecular Imager® ChemiDoc™ XRS system (Bio-Rad Laboratories, Inc.). The primary antibodies used in this study were as follows: Cleaved caspase-3 (1:1,000; cat. no. 9664), caspase-3 (1:1,000; cat. no. 9662), Bax (1:1,000; cat. no. 2772), E-cadherin (1:1,000; cat. no. 14472), N-cadherin (1:1,000; cat. no. 13116), vimentin (1:1,000; cat. no. 5741), β-catenin (1:1,000; cat. no. 8480), cyclin D1 (1:500; cat. no. 55506), C-myc (1:1,000; cat. no. 18583) and GAPDH (1:1,000; cat. no. 5174) (all from Cell Signaling Technology, Inc.); Bcl-2 (1:1,000; cat. no. ab32124), matrix metalloprotease (MMP)-2 (1:1,000; cat. no. ab97779), MMP-9 (1:1,000; cat. no. ab76003), and FZD1 (1:500; cat. no. ab83044) (all from Abcam).

Tumor formation assay in a nude mouse model. A total of 12 athymic BALB/c female nude mice (age, 4 weeks; weight, 18-22 g) were supplied by the Laboratory Animal Centre of Chinese Academy of Sciences. The procedures employed

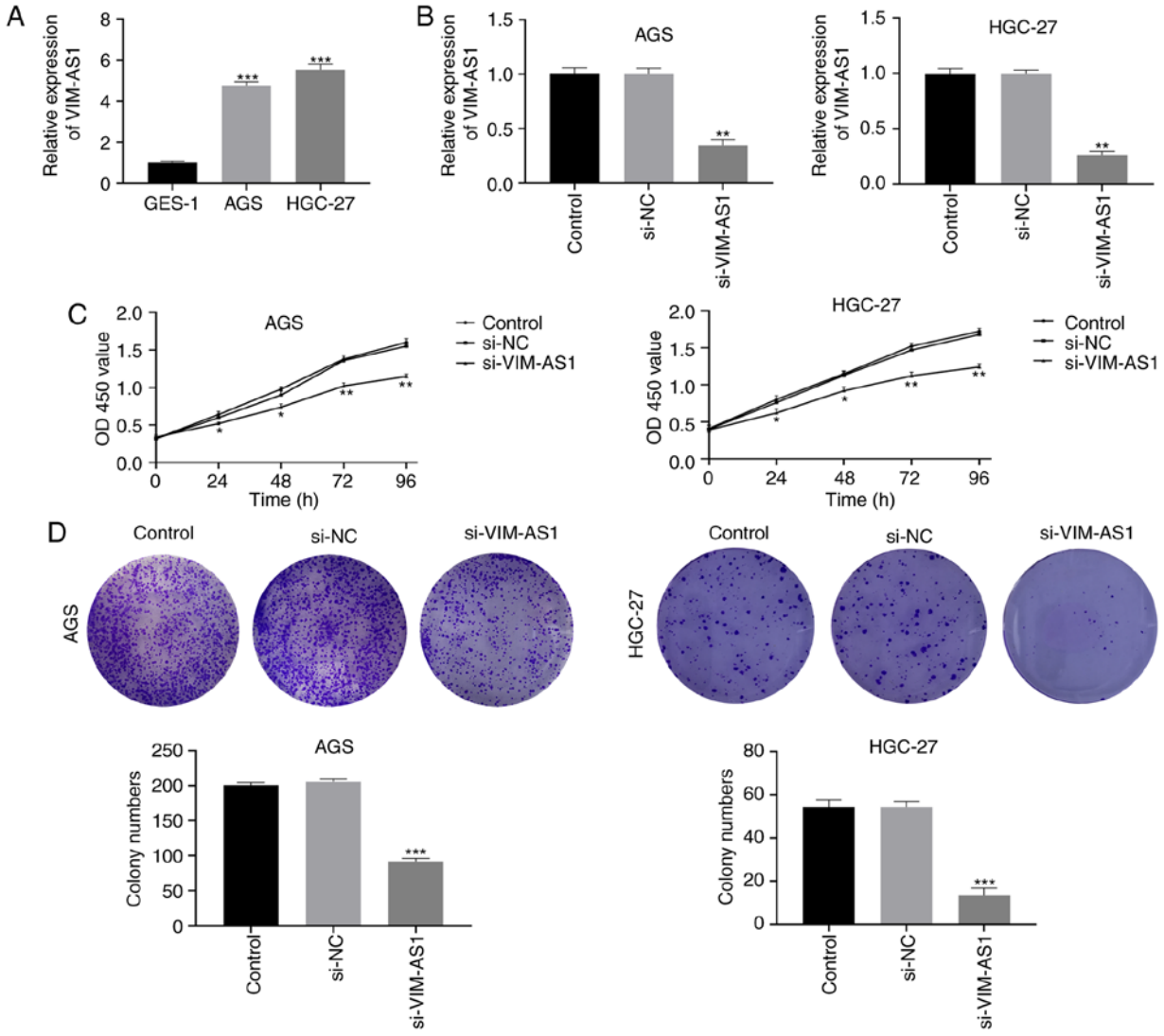

Figure 2. Silencing VIM-AS1 inhibits the proliferation of AGS and HGC-27 cells. (A) VIM-AS1 expression was detected by RT-qPCR in GES-1, AGS and HGC-27 cells. **P<0.01, ***P<0.001 vs. GES-1. (B) VIM-AS1 expression was detected in transfected AGS and HGC-27 cells by reverse transcription-quantitative PCR. (C) Proliferation of AGS and HGC-27 cells was measured by Cell Counting Kit-8 assay. (D) Numbers of AGS and HGC-27 cell colonies were detected by colony formation assay. *P<0.05, **P<0.01, ***P<0.001 vs. si-NC group. VIM-AS1, VIM antisense RNA 1; si, small interfering RNA; NC, negative control; OD, optical density.

for the animal studies were approved by the Animal Use Committee of Shouguang People's Hospital. All mice were housed in a temperature-controlled environment (23±2˚C), with 50±5% humidity, under a 12-h light/dark cycle and were provided with free access to food and water. The mice were randomly assigned to two groups (n=6 mice/group). Briefly, HGC-27 cells ($1x10^7$ cells/mouse) transfected with si-VIM-AS1 or si-NC were subcutaneously injected into the right dorsal flank of BABL/c nude mice. The tumor volume was determined every 5 days using the following formula: Volume=length x $width^2$ x1/2. After 25 days, the mice were euthanized with 100 mg/kg (1.5%) sodium pentobarbital by tail vein injection and xenograft tumor weights were recorded. In addition, the humane endpoint was that mice were sacrificed when tumor size reached 2,000 mm^3. None of the mice were sacrificed during the 25 days.

Statistical analysis. All experimental data from triplicate experiments were expressed as the mean ± standard error of the mean. The significance differences between two groups were analyzed using a paired Student's t-test or one-way ANOVA followed by Tukey's multiple comparison post hoc test for multiple groups. Survival rates were assessed by the Kaplan-Meier method, and survival curves were compared by log-rank tests. All statistical analyses were performed using SPSS 23.0 Statistical Software (IBM Corp.). P<0.05 was considered to indicate a statistically significant difference.

Results

VIM-AS1 expression is upregulated in GC tissues and associated with the prognosis of GC. The association between VIM-AS1 expression and clinicopathological features was reported in Table I. The data indicated that the expression of VIM-AS1 in patients with GC was significantly associated with TNM stages (P<0.001), lymph node metastasis (P<0.001) and distant metastasis

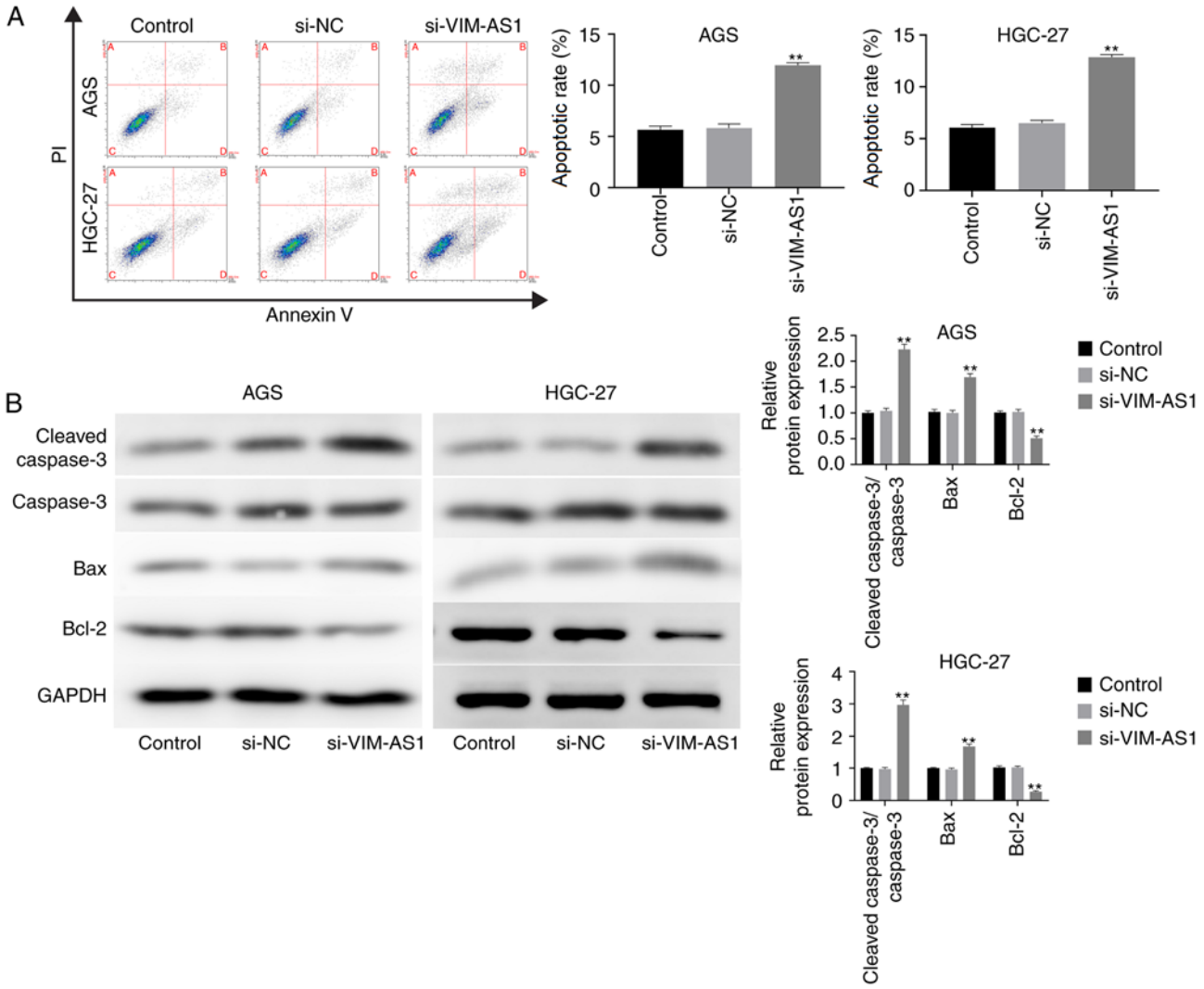

Figure 3. Silencing VIM-AS1 promotes apoptosis of AGS and HGC-27 cells. (A) Apoptotic rate of AGS and HGC-27 cells was measured by flow cytometry. (B) Protein expression levels of cleaved caspase-3, caspase-3, Bax and Bcl-2 was measured by western blotting. **P<0.01 vs. si-NC group. VIM-AS1, VIM antisense RNA 1; si, small interfering RNA; NC, negative control; PI, propidium iodide.

(P<0.001; Table I). However, no significant association was observed between the expression of VIM-AS1 and other clinical characteristics, such as age, sex, tumor size and histological differentiation (Table I). To further evaluate the association between VIM-AS1 and GC, RT-qPCR was performed to explore the expression of VIM-AS1 in GC tissues. RT-qPCR results demonstrated that the expression levels of VIM-AS1 in GC tissues were significantly higher compared with those in cancer-adjacent tissues (P<0.001; Fig. 1A). The expression of VIM-AS1 was also significantly increased in stage III/IV cancer tissues compared with in stage I/II cancer tissues (P<0.001; Fig. 1B). In addition, the expression of VIM-AS1 was significantly upregulated in tissues from patients with lymph node metastasis and distant metastasis compared with in those from patients without metastasis (P<0.001; Fig. 1C and D). In addition, the patients with low VIM-AS1 expression had significantly longer overall survival compared with patients with high VIM-AS1 expression (P<0.01; Fig. 1E). These results suggested that VIM-AS1 upregulation may be associated with the progression of GC.

Silencing VIM-AS1 inhibits proliferation of AGS and HGC-27 cells. To further investigate the effect of VIM-AS1 on GC *in vitro*, the expression levels of VIM-AS1 were measured in GC cell lines. The results demonstrated that the expression of VIM-AS1 was significantly elevated in AGS and HGC-27 cells compared with that in GES-1 cells (P<0.001; Fig. 2A). Thus, si-VIM-AS1 and si-NC were transfected into AGS and HGC-27 cells (Fig. 2B). The results demonstrated that VIM-AS1 expression in the si-VIM-AS1 group was significantly higher compared with that in the si-NC group (P<0.01; Fig. 2B), which indicated that the transfection was successful. Subsequently, the effects of VIM-AS1 on GC cell proliferation were detected by CCK-8 and colony formation assays. The results of the CCK-8 assay demonstrated that silencing VIM-AS1 significantly suppressed the proliferation of AGS and HGC-27 cells 24 (P<0.05), 48 (P<0.05), 72 (P<0.01) and 96 h (P<0.01) post-transfection (Fig. 2C). In addition, colony formation assay demonstrated that the numbers of AGS and HGC-27 cell colonies were significantly decreased in the si-VIM-AS1 group compared with those in the si-NC group (P<0.001; Fig. 2D). These results suggested that silencing

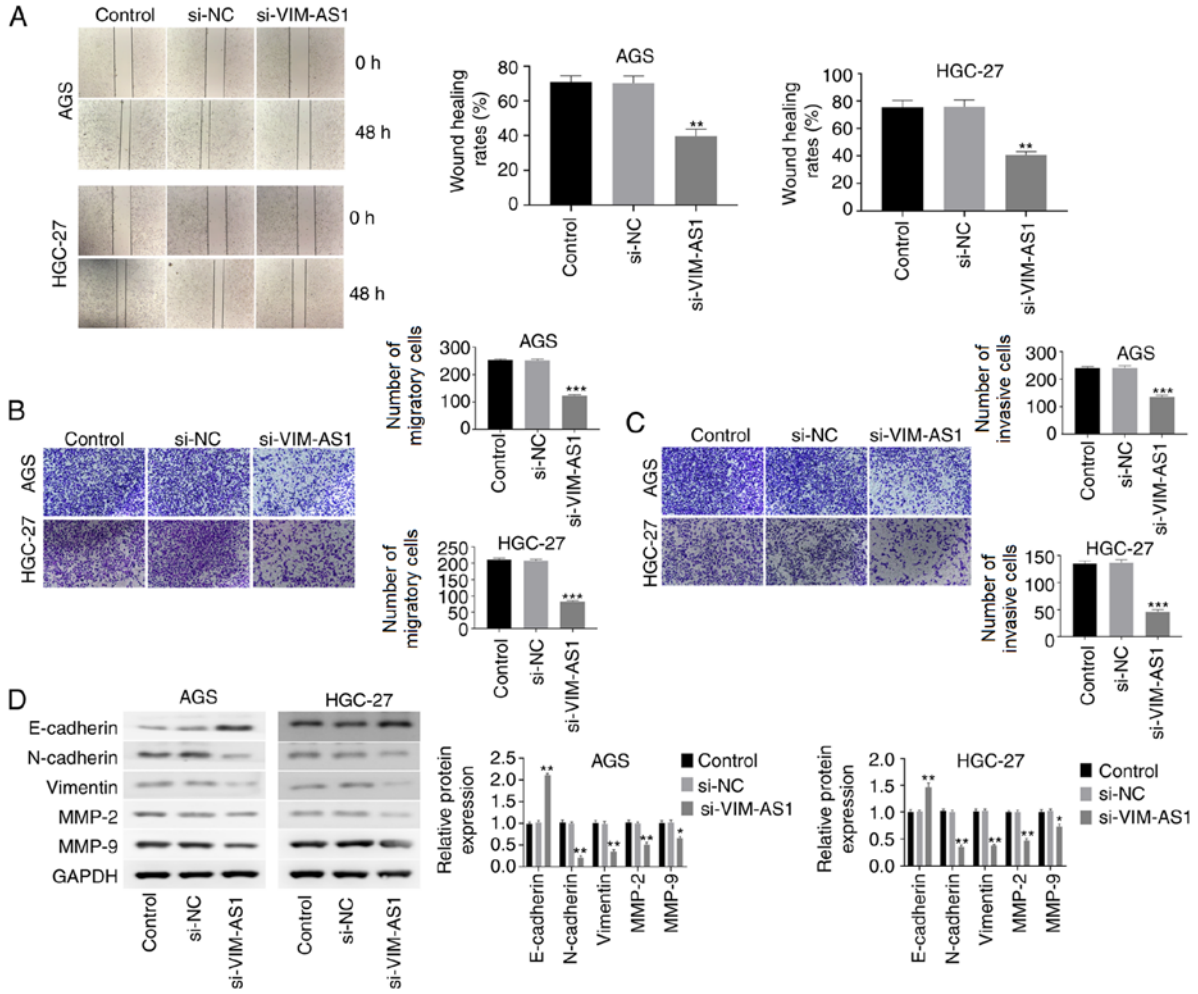

Figure 4. Silencing VIM-AS1 inhibits the migration, invasion and EMT of AGS and HGC-27 cells. (A) Wound-healing assay was used to investigate the migratory ability of AGS and HGC-27 cells (magnification, x40). (B) Transwell assay was performed to detect the migratory ability of AGS and HGC-27 cells (magnification, x100). (C) Transwell assay was performed to detect the invasive ability of AGS and HGC-27 cells (magnification, x100). (D) Protein expression levels of E-cadherin, N-cadherin, vimentin, MMP-2 and MMP-9 were measured by western blotting. *P<0.05, **P<0.01, ***P<0.001 vs. si-NC group. VIM-AS1, VIM antisense RNA 1; si, small interfering RNA; NC, negative control; MMP, matrix metalloproteinase.

VIM-AS1 suppressed the proliferative ability of AGS and HGC-27 cells.

Silencing VIM-AS1 promotes apoptosis of AGS and HGC-27 cells. To investigate the effect of VIM-AS1 on GC cell apoptosis, flow cytometry was performed. The results demonstrated that the apoptotic rate of AGS and HGC-27 cells was significantly enhanced in the si-VIM-AS1 group compared with that in the si-NC group (P<0.01; Fig. 3A). In addition, the results of western blotting demonstrated that silencing VIM-AS1 significantly increased the expression levels of cleaved caspase-3/caspase-3 and Bax, but decreased Bcl-2 expression levels in AGC and HGC-27 cells compared with those in the si-NC group (P<0.01; Fig. 3B). These results suggested that silencing VIM-AS1 facilitated the apoptotic ability of AGC and HGC-27 cells.

Silencing VIM-AS1 inhibits migration, invasion and EMT in AGS and HGC-27 cells. The results of the wound-healing assay demonstrated that cell migration was significantly inhibited in si-VIM-AS1-transfected AGC and HGC-27 cells compared with that in the si-NC-transfected cells (P<0.01; Fig. 4A). The Transwell assay revealed that silencing VIM-AS1 significantly reduced the extent of migration and invasion of AGC and HGC-27 cells compared with in the si-NC group (P<0.001; Fig. 4B and C). It has been reported that EMT serves an important role in the migration and invasion of GC cells (19). Therefore, the effect of VIM-AS1 on EMT in AGC and HGC-27 cells was investigated. The results of western blotting demonstrated that silencing VIM-AS1 significantly elevated E-cadherin expression (P<0.01), but reduced the expression of N-cadherin (P<0.01), vimentin (P<0.01), MMP-2 (P<0.01) and MMP-9 (P<0.05) in AGC and HGC-27 cells compared with those in the si-NC group (Fig. 4D). These results suggested that silencing VIM-AS1 inhibited migration, invasion and EMT in AGS and HGC-27 cells.

Silencing VIM-AS1 inhibits the expression of FZD1 in AGS and HGC-27 cells. Compared with in the mimics NC or inhibitor NC group, transfection with miR-8052 mimics significantly increased miR-8052 expression in AGS and HGC-27 cells, whereas transfection with the miR-8052 inhibitor significantly decreased miR-8052 expression, thus indicating that miR-8052

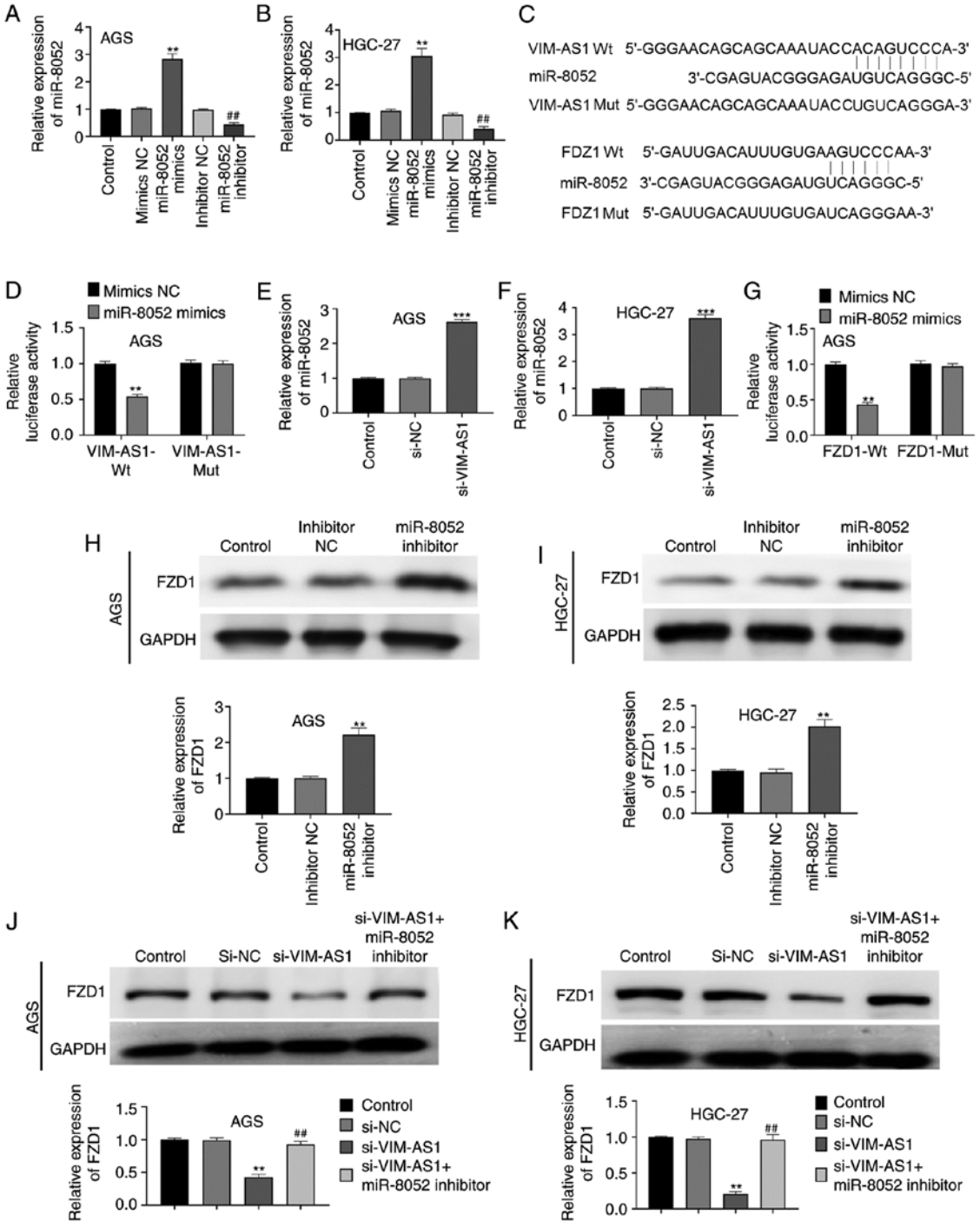

Figure 5. Silencing VIM-AS1 inhibits the expression of FZD1 in AGS and HGC-27 cells. miR-8052 expression in transfected (A) AGS and (B) HGC-27 cells was detected by RT-qPCR. **P<0.01 vs. mimics NC group; $^{\#\#}$P<0.01 vs. inhibitor NC group. (C) Binding sites between VIM-AS1, miR-8052 and FZD1 were predicted by TargetScan 7.2 and DIANA tools. (D and G) Luciferase activity was determined by dual luciferase reporter gene assay. **P<0.01 vs. mimics NC group. miR-8052 expression was detected in (E) AGS and (F) HGC-27 cells by RT-qPCR. ***P<0.001 vs. si-NC group. (H and I) Expression of FZD1 was measured in AGS and HGC-27 cells transfected with miR-8052 inhibitor and inhibitor NC by western blotting. **P<0.01 vs. inhibitor NC group. (J and K) Expression of FZD1 was measured in AGS and HGC-27 cells transfected with si-NC, si-VIM-AS1 and si-VIM-AS1 + miR-8052 inhibitor by western blotting. **P<0.01 vs. si-NC group; $^{\#\#}$P<0.01 vs. si-VIM-AS1 group. VIM-AS1, VIM antisense RNA 1; FZD1, frizzled 1; RT-qPCR, reverse transcription-quantitative PCR; si, small interfering RNA; NC, negative control; miR; micro RNA; Wt, wild-type; Mut, mutant.

mimics and miR-8052 inhibitor were successfully transfected into AGS and HGC-27 cells (P<0.01; Fig. 5A and B). The binding sites between VIM-AS1, miR-8052 and FZD1 were predicted using TargetScan 7.2 and DIANA tools (Fig. 5C). In addition, dual luciferase reporter gene assay demonstrated that compared with in the mimics NC group, miR-8052 mimics significantly reduced luciferase activity in the VIM-AS1-Wt (P<0.01) and FZD1-Wt groups (P<0.01), but had no significant effect on the luciferase activity in the VIM-AS1-Mut and FZD1-Mut groups (P>0.05; Fig. 5D and G). Additionally, silencing VIM-AS1 significantly elevated the expression levels of miR-8052 in AGS and HGC-27 cells compared with those in

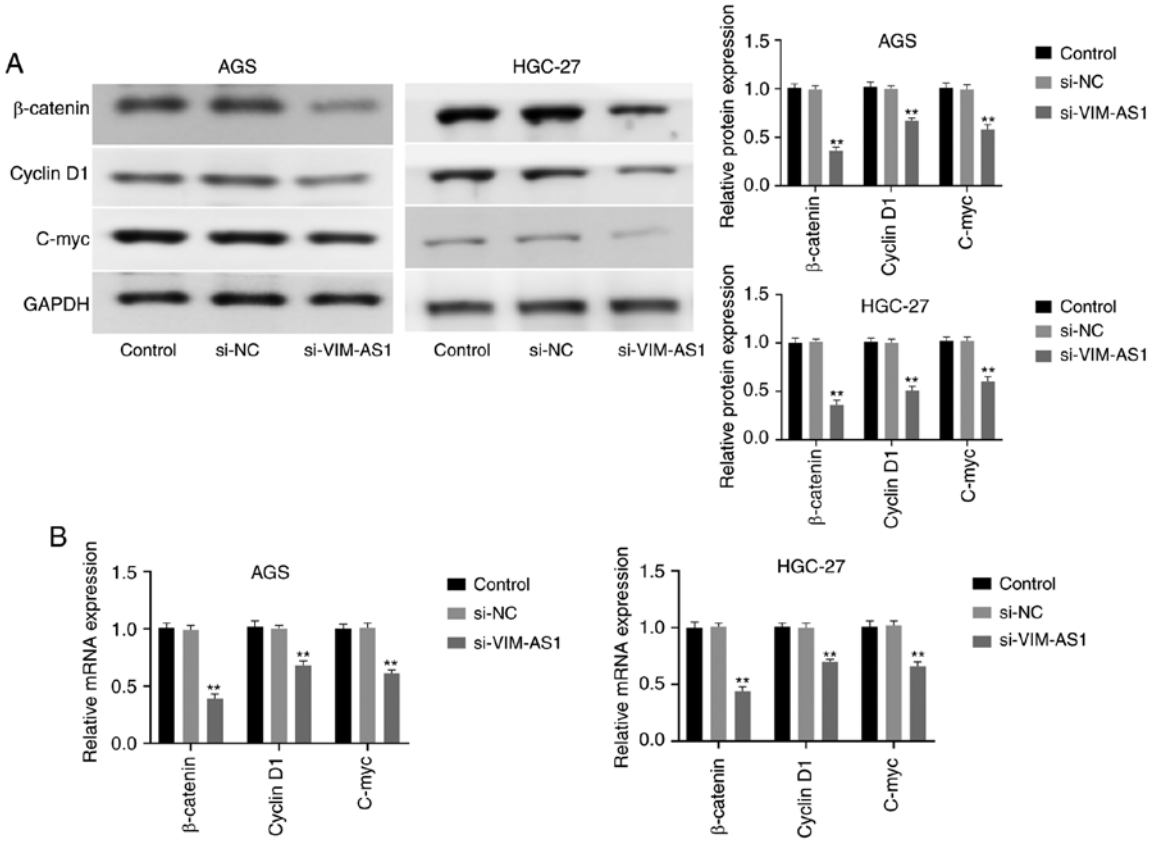

Figure 6. Silencing VIM-AS1 suppresses the Wnt/β-catenin pathway in AGS and HGC-27 cells. (A) Protein expression levels of β-catenin, cyclin D1 and C-myc were measured by western blotting. (B) mRNA expression levels of β-catenin, cyclin D1 and C-myc was measured by reverse transcription-quantitative PCR. **P<0.01 vs. si-NC group. VIM-AS1, VIM antisense RNA 1; si, small interfering RNA; NC, negative control.

the si-NC group (P<0.001; Fig. 5E and F). To further confirm the relationship among VIM-AS1, miR-8052 and FZD1, western blotting was performed. The results demonstrated that the knockdown of miR-8052 significantly increased the expression levels of FDZ1 in AGS and HGC-27 cells compared with those in the inhibitor NC group (P<0.01; Fig. 5H and I). In addition, silencing VIM-AS1 significantly decreased FZD1 expression in AGS and HGC-27 cells compared with those in the si-NC group (P<0.01; Fig. 5J and K). Notably, co-transfection of cells with si-VIM-AS1 and miR-8052 inhibitor significantly reversed the effect of VIM-AS1 silencing on FZD1 expression in AGS and HGC-27 cells (P<0.01; Fig. 5J and K). These results suggested that silencing VIM-AS1 inhibited the expression of FZD1 in AGS and HGC-27 cells.

Silencing VIM-AS1 suppresses the Wnt/β-catenin pathway in AGS and HGC-27 cells. To explore the effects of VIM-AS1 on the Wnt/β-catenin pathway, the expression levels of β-catenin, cyclin D1 and C-myc were measured by western blotting and RT-qPCR after silencing VIM-AS1 in AGS and HGC-27 cells. The results demonstrated that silencing VIM-AS1 significantly decreased the protein expression levels of β-catenin (P<0.01), cyclin D1 (P<0.01) and C-myc (P<0.01) in AGC and HGC-27 cells compared with those in the si-NC group (Fig. 6A). In addition, RT-qPCR confirmed that silencing VIM-AS1 significantly decreased the mRNA expression levels of β-catenin (P<0.01), cyclin D1 (P<0.01) and C-myc (P<0.01) compared with those in the si-NC group (Fig. 6B). These results suggested that silencing VIM-AS1 suppressed the Wnt/β-catenin pathway in AGS and HGC-27 cells.

Silencing VIM-AS1 inhibits tumor growth in nude mice. To explore whether VIM-AS1 affects tumorigenesis, HGC-27 cells transfected with si-VIM-AS1 or si-NC were used in a nude mice xenograft model (Fig. 7A). The results demonstrated that tumor volume was significantly smaller and the weight of xenograft tumors was significantly lighter in the si-VIM-AS1 group compared with in the si-NC group (P<0.01; Fig. 7B and C). These results suggested that silencing VIM-AS1 inhibited tumor growth in nude mice.

Discussion

GC is one of the main causes of cancer-related death in China (20). Patients with GC that present with distant metastasis often have a poor prognosis, and are unable to undergo optimal and timely surgical intervention. Thus, it is important to search for innovative, novel and effective targets to improve prognostic and therapeutic strategies for GC. The results of the present study suggested that VIM-AS1 promoted cell proliferation, migration, invasion and EMT by regulating FDZ1 and activating the Wnt/β-catenin pathway in GC.

Accumulating evidence has suggested that lncRNAs are involved in diverse biological processes by modulating gene expression (21). Recently, lncRNAs have been reported to

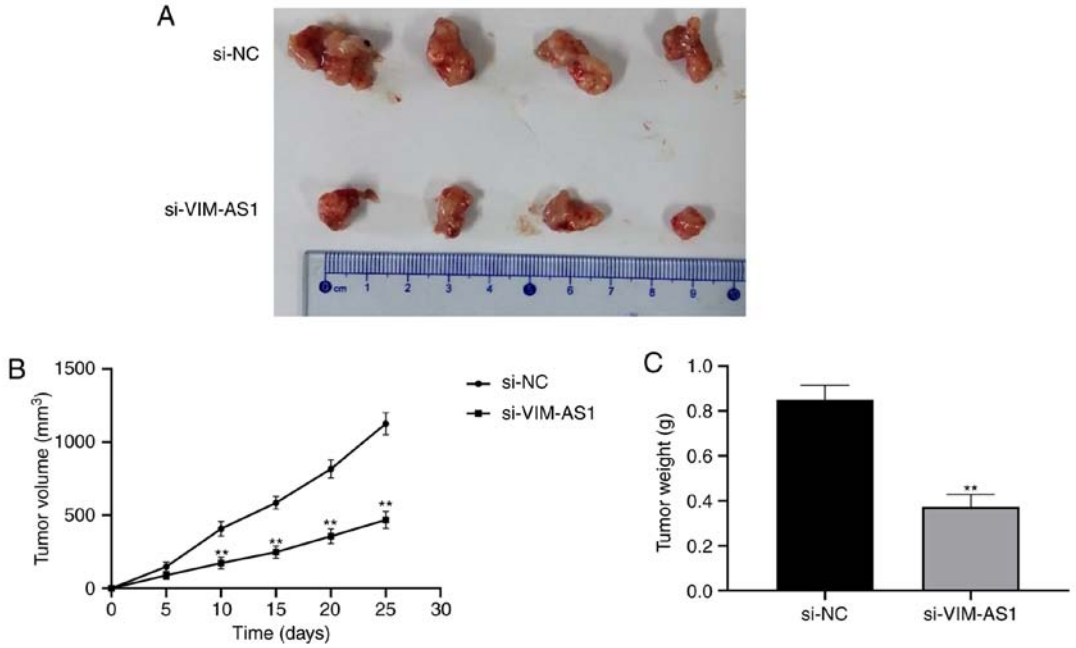

Figure 7. Silencing VIM-AS1 inhibits tumor growth in nude mice. (A) Representative images of xenograft tumors. (B) Tumor volume of the xenografts in si-VIM-AS1 and si-NC groups. (C) Tumor weight of the xenografts in si-VIM-AS1 and si-NC groups. **P<0.01 vs. si-NC group. VIM-AS1, VIM antisense RNA 1; si, small interfering RNA; NC, negative control.

serve important roles in the progression of numerous tumor types (22). Although VIM-AS1 is characterized as an oncogene in colorectal cancer (12), to the best of our knowledge, its relationship with GC has not been reported. In the present study, VIM-AS1 was demonstrated to be highly expressed in GC tissues and cell lines (AGS and HGC-27 cells). In addition, the expression of VIM-AS1 was associated with the prognosis of GC and some clinical parameters, including TNM stage, lymph node metastasis and distant metastasis. The results of the present study suggested that VIM-AS1 may serve as an oncogene in GC. A previous study confirmed that lncRNAs may be involved in regulating cell proliferation, apoptosis, migration and invasion in GC (23). A recent study demonstrated that hepatocellular carcinoma upregulated lncRNA promoted the proliferation, migration and invasion of GC cells via regulation of the miR-9-5p/myosin heavy chain 9 axis (24). Another study observed that the lncRNA amine oxidase copper containing 4, pseudogene affected the biological behavior of GC cells by modulating the mitogen-activated protein kinase pathway (25). In addition, Wang *et al* (26) demonstrated that the lncRNA small nucleolar RNA host gene 7 promoted the proliferation and inhibited the apoptosis of GC cells through regulation of p15 and p16 expression. The present study investigated the role of VIM-AS1 expression in GC cells and demonstrated that silencing VIM-AS1 significantly inhibited the proliferation, migration and invasion, and enhanced the apoptosis of AGS and HGC-27 cells. Additionally, western blotting results demonstrated that silencing VIM-AS1 promoted the expression of cleaved caspase-3 and Bax in AGS and HGC-27 cells, but suppressed the expression of Bcl-2, which further suggested that silencing VIM-AS1 may promote GC cells apoptosis.

EMT is a crucial step in the progression of cancer cell metastasis, which is characterized by the loss of epithelial features and the acquisition of mesenchymal features by cells (27). Notably, the expression of the epithelial marker E-cadherin is decreased in cancer cells during the process of EMT, whereas the expression of mesenchymal markers N-cadherin and vimentin is increased (28). In addition, a previous study demonstrated that MMPs, including MMP-2 and MMP-9, which enhance the invasion and metastasis of tumor cells, are highly expressed during the process of EMT (29). The results of the present study demonstrated that silencing VIM-AS1 increased E-cadherin expression, and reduced the expression levels of N-cadherin, vimentin, MMP-2 and MMP-9, which supported the hypothesis that silencing VIM-AS1 suppressed the process of EMT in GC cells. In addition, the results of the present study demonstrated that silencing VIM-AS1 inhibited tumorigenesis *in vivo*.

The Wnt/β-catenin pathway serves an important role in a various types of cancer as it regulates numerous processes, such as cell proliferation, apoptosis, migration and invasion (30). The Wnt receptor FZD1 is considered to be an essential component of the Wnt/β-catenin pathway, and has been observed to be overexpressed in neuroblastoma and breast cancer (30,31). Numerous studies have also demonstrated that overactivation of the Wnt/β-catenin pathway is attributable to the overexpression of FZD receptors in several types of cancer (32,33). In addition, the Wnt/β-catenin pathway regulates its downstream target genes, such as cyclin D1 and C-myc during the progression of cancer (34). β-catenin is reported to be a critical molecule involved in the Wnt/β-catenin signaling pathway in the extracellular ligands of tumor cells (35). Several studies have demonstrated that lncRNAs may modulate the biological behaviors of GC cells by regulating the Wnt/β-catenin pathway. For example, LINC00052 has been reported to promote GC cell proliferation and metastasis through activation of the Wnt/β-catenin pathway (36). Peng *et al* (16) suggested that

growth arrest-associated lncRNA 1 suppressed the growth of GC by inhibiting activation of the Wnt/β-catenin pathway. Wang *et al* (17) reported that knockdown of lncRNA TP73-AS1 inhibited GC cell proliferation and invasion through regulating the Wnt/β-catenin pathway. The results of the present study demonstrated that silencing VIM-AS1 significantly inhibited FZD1 expression by targeting miR-8052. In addition, silencing VIM-AS1 significantly reduced the protein and mRNA expression levels of β-catenin, cyclin D1 and C-myc in AGS and HGC-27 cells, which together suggested that silencing VIM-AS1 may inhibit GC cell proliferation, migration, invasion and EMT in GC cells by downregulating FZD1 and inactivating the Wnt/β-catenin pathway. Notably, further studies are required to identify other potential mechanisms of VIM-AS1 that are involved in GC progression *in vitro*, as well as the role of VIM-AS1 and its underlying molecular mechanisms in GC *in vivo*.

In conclusion, the results of the present study demonstrated that VIM-AS1 was highly expressed in GC tissues and cell lines, and that VIM-AS1 promoted cell proliferation, migration, invasion and EMT possibly by regulating FDZ1 and activating the Wnt/β-catenin pathway in GC. These findings support the oncogenic role of VIM-AS1 in GC, which may encourage studies on VIM-AS1 as a potentially diagnostic biomarker and therapeutic target for GC.

Acknowledgements

Not applicable.

Funding

No funding was received.

Availability of data and materials

The datasets used and/or analyzed during the current study are available from the corresponding author on reasonable request.

Authors' contributions

XFL designed the study. JGS, XBL and RHY performed the experiments and analyzed the data. JGS wrote the manuscript. All authors read and approved the final manuscript.

Ethics approval and consent to participate

This study involving human samples was approved by the Ethics Committee of Shouguang People's Hospital (approval no. 201803). All patients provided written informed consent. The procedures employed for the animal studies were approved by the Animal Use Committee of Shouguang People's Hospital.

Patient consent for publication

Not applicable.

Competing interests

The authors declare that they have no competing interests.

References

1. Siegel RL, Miller KD and Jemal A: Cancer statistics, 2017. CA Cancer J Clin 67: 7-30, 2017.
2. Zheng S, Lv P, Su J, Miao K, Xu H and Li M: Silencing of the long non-coding RNA RHPN1-AS1 suppresses the epithelial-to-mesenchymal transition and inhibits breast cancer progression. Am J Transl Res 11: 3505-3517, 2019.
3. Dong Y, Wang ZG and Chi TS: Long noncoding RNA Lnc01614 promotes the occurrence and development of gastric cancer by activating EMT pathway. Eur Rev Med Pharmacol Sci 22: 1307-1314, 2018.
4. Batista PJ and Chang HY: Long noncoding RNAs: Cellular address codes in development and disease. Cell 152: 1298-1307, 2013.
5. Hirano T, Yoshikawa R, Harada H, Harada Y, Ishida A and Yamazaki T: Long noncoding RNA, CCDC26, controls myeloid leukemia cell growth through regulation of KIT expression. Mol Cancer 14: 90, 2015.
6. Prensner JR, Iyer MK, Balbin OA, Dhanasekaran SM, Cao Q, Brenner JC, Laxman B, Asangani IA, Grasso CS, Kominsky HD, *et al*: Transcriptome sequencing across a prostate cancer cohort identifies PCAT-1, an unannotated lincRNA implicated in disease progression. Nat Biotechnol 29: 742-749, 2011.
7. Tordonato C, Di Fiore PP and Nicassio F: The role of non-coding RNAs in the regulation of stem cells and progenitors in the normal mammary gland and in breast tumors. Front Genet 6: 72, 2015.
8. Lin XC, Zhu Y, Chen WB, Lin LW, Chen DH, Huang JR, Pan K, Lin Y, Wu BT, Dai Y and Tu ZG: Integrated analysis of long non-coding RNAs and mRNA expression profiles reveals the potential role of lncRNAs in gastric cancer pathogenesis. Int J Oncol 45: 619-628, 2014.
9. Cao WJ, Wu HL, He BS, Zhang YS and Zhang ZY: Analysis of long non-coding RNA expression profiles in gastric cancer. World J Gastroenterol 19: 3658-3664, 2013.
10. Liu D, Zhang MY, Chu Z and Zhang M: Long non-coding RNA HOST2 enhances proliferation and metastasis in gastric cancer. Neoplasma 66: 101-108, 2019.
11. Pan L, Liang W, Gu J, Zang X, Huang Z, Shi H, Chen J, Fu M, Zhang P, Xiao X, *et al*: Long noncoding RNA DANCR is activated by SALL4 and promotes the proliferation and invasion of gastric cancer cells. Oncotarget 9: 1915-1930, 2018.
12. Rezanejad Bardaji H, Asadi MH and Yaghoobi MM: Long noncoding RNA VIM-AS1 promotes colorectal cancer progression and metastasis by inducing EMT. Eur J Cell Biol 97: 279-288, 2018.
13. Zhao X, Jiang X, Liu Z, Zhou M, Zhang J, Wang X and Li X: Long noncoding RNA VIM antisense RNA 1 (VIM-AS1) plays an important role in development of preeclampsia by regulation of epithelial mesenchymal transition. Med Sci Monit 25: 8306-8314, 2019.
14. Clevers H and Nusse R: Wnt/β-catenin signaling and disease. Cell 149: 1192-1205, 2012.
15. Han P, Li JW, Zhang BM, Lv JC, Li YM, Gu XY, Yu ZW, Jia YH, Bai XF, Li L, *et al*: The lncRNA CRNDE promotes colorectal cancer cell proliferation and chemoresistance via miR-181a-5p-mediated regulation of Wnt/beta-catenin signaling. Mol Cancer 16: 9, 2017.
16. Peng C, Li X, Yu Y and Chen J: LncRNA GASL1 inhibits tumor growth in gastric carcinoma by inactivating the Wnt/β-catenin signaling pathway. Exp Ther Med 17: 4039-4045, 2019.
17. Wang Y, Xiao S, Wang B, Li Y and Chen Q: Knockdown of lncRNA TP73-AS1 inhibits gastric cancer cell proliferation and invasion via the WNT/β-catenin signaling pathway. Oncol Lett 16: 3248-3254, 2018.
18. Livak KJ and Schmittgen TD: Analysis of relative gene expression data using real-time quantitative PCR and the 2(-Delta Delta C(T)) method. Methods 25: 402-408, 2001.
19. Huang L, Wu RL and Xu AM: Epithelial-mesenchymal transition in gastric cancer. Am J Transl Res 7: 2141-2158, 2015.
20. Chen W, Zheng R, Baade PD, Zhang S, Zeng H, Bray F, Jemal A, Yu XQ and He J: Cancer statistics in China, 2015. CA Cancer J Clin 66: 115-132, 2016.
21. Ponting CP, Oliver PL and Reik W: Evolution and functions of long noncoding RNAs. Cell 136: 629-641, 2009.
22. Renganathan A and Felley-Bosco E: Long noncoding RNAs in cancer and therapeutic potential. Adv Exp Med Biol 1008: 199-222, 2017.

23. He C, Yang W, Yang J, Ding J, Li S, Wu H, Zhou F, Jiang Y, Teng L and Yang J: Long noncoding RNA MEG3 negatively regulates proliferation and angiogenesis in vascular endothelial cells. DNA Cell Biol 36: 475-481, 2017.
24. Liu T, Liu Y, Wei C, Yang Z, Chang W and Zhang X: LncRNA HULC promotes the progression of gastric cancer by regulating miR-9-5p/MYH9 axis. Biomed Pharmacother 121: 109607, 2019.
25. Qu CX, Shi XC, Bi H, Zhai LQ and Yang Q: LncRNA AOC4P affects biological behavior of gastric cancer cells through MAPK signaling pathway. Eur Rev Med Pharmacol Sci 23: 8852-8860, 2019.
26. Wang MW, Liu J, Liu Q, Xu QH, Li TF, Jin S and Xia TS: LncRNA SNHG7 promotes the proliferation and inhibits apoptosis of gastric cancer cells by repressing the P15 and P16 expression. Eur Rev Med Pharmacol Sci 21: 4613-4622, 2017.
27. De Craene B and Berx G: Regulatory networks defining EMT during cancer initiation and progression. Nat Rev Cancer 13: 97-110, 2013.
28. Singh A and Settleman J: EMT, cancer stem cells and drug resistance: An emerging axis of evil in the war on cancer. Oncogene 29: 4741-4751.
29. Coussens LM, Fingleton B and Matrisian LM: Matrix metalloproteinase inhibitors and cancer-trials and tribulations. Science 295: 2387-2392, 2002.
30. Flahaut M, Meier R, Coulon A, Nardou KA, Niggli FK, Martinet D, Beckmann JS, Joseph JM, Mühlethaler-Mottet A and Gross N: The Wnt receptor FZD1 mediates chemoresistance in neuroblastoma through activation of the Wnt/beta-catenin pathway. Oncogene 28: 2245-2256, 2009.
31. Zhang H, Zhang X, Wu X, Li W, Su P, Cheng H, Xiang L, Gao P and Zhou G: Interference of Frizzled 1 (FZD1) reverses multidrug resistance in breast cancer cells through the Wnt/β-catenin pathway. Cancer Lett 323: 106-113, 2012.
32. Milovanovic T, Planutis K, Nguyen A, Marsh JL, Lin F, Hope C and Holcombe RF: Expression of Wnt genes and frizzled 1 and 2 receptors in normal breast epithelium and infiltrating breast carcinoma. Int J Oncol 25: 1337-1342, 2004.
33. Merle P, Kim M, Herrmann M, Gupte A, Lefrançois L, Califano S, Trépo C, Tanaka S, Vitvitski L, de la Monte S and Wands JR: Oncogenic role of the frizzled-7/beta-catenin pathway in hepatocellular carcinoma. J Hepatol 43: 854-862, 2005.
34. Ara H, Takagishi M, Enomoto A, Asai M, Ushida K, Asai N, Shimoyama Y, Kaibuchi K, Kodera Y and Takahashi M: Role for Daple in non-canonical Wnt signaling during gastric cancer invasion and metastasis. Cancer Sci 107: 133-139, 2016.
35. Karimaian A, Majidinia M, Bannazadeh Baghi H and Yousefi B: The crosstalk between Wnt/β-catenin signaling pathway with DNA damage response and oxidative stress: Implications in cancer therapy. DNA Repair (Amst) 51: 14-19, 2017.
36. Shan Y, Ying R, Jia Z, Kong W, Wu Y, Zheng S and Jin H: LINC00052 promotes gastric cancer cell proliferation and metastasis via activating the Wnt/β-catenin signaling pathway. Oncol Res 25: 1589-1599, 2017.